Journal of Engineering Physics and Thermophysics, Vol. 83, No. 6, 2010

FORMATION OF A DETONATION WAVE IN THE PROCESS OF CHEMICAL CONDENSATION OF CARBON NANOPARTICLES

A. V. Emel'yanov, A. V. Eremin, and V. E. Fortov

UDC 539.3:621.374

A new physical phenomenon — the formation of a detonation wave as a result of the condensation of substances — was investigated in detail. A detonation wave was formed under the action of the energy released in a process of chemical condensation of carbon nanoparticles behind a shock wave in the mixture initially containing 10–30% of the carbon suboxide C_3O_2 or acetylene C_2H_2 in argon. The propagation of the shock wave in this mixture led to the rapid thermal disintegration of its initial molecules and the subsequent formation of a condensed carbon with a significant energy release. The increase in the temperature and in the pressure of the reacting mixture leads to a strengthening of the shock wave and to its transformation into a detonation wave. The main kinetic characteristics of the reaction of thermal disintegration of the indicated molecules and their subsequent chemical condensation as well as the interrelation of these characteristics with the heat-release processes forming the detonation wave were determined.

Keywords: *detonation wave, chemical condensation of carbon nanoparticles, shock and detonation waves, thermal deisintegration of molecules.*

Introduction. It is well known that the detonation of the majority of gaseous hydrocarbon fuels is accompanied by the formation of condensed carbon particles and that the condensation process, like the oxidation reaction, proceeds with great heat release. The most characteristic process of such kind is the self-decomposition of acetylene that, even with no an oxidizer (i.e., in the absence of combustion), has a fairly significant positive heat balance [1]:

$$C_2H_2 \rightarrow 2C(\text{graphite}) + H_2 \quad (+ 277 \text{ kJ/mole}) . \tag{1}$$

The process of detonation self-decomposition of acetylene was first described as far back as 1899 by Berthélot and Le Chatelier [2]. However, it is known that this effect arises only at high pressures [1, 3, 4]; moreover, the contribution of the condensation energy to the formation of a detonation wave in the indicated process is difficult to determine quantitatively because of the presence of a large number of complex intermediate reactions of growth of polyatomic polycyclic hydrocarbons preceding the formation of condensed carbon particles. Nevertheless, it is well known that the heat of condensation of carbon vapor is fairly large and comprises 716 kJ/mole. This raises the entirely natural question of whether a detonation wave can be initiated by only the condensation energy.

In [5], Landau described a condensation shock arising as a result of an abrupt expansion and cooling of the vapor in a supersonic jet. However, even though this shock is formally identical to the detonation wave, it does not transform a supersonic flow into a subsonic one and, strictly speaking, is not a detonation wave. In other words, Landau investigated the condensation heat release without account for the fact that a detonation wave is formed and sustained under the action of this heat energy.

In the present work, we propose a somewhat different experiment that makes it possible to realize conditions for the appearance of a condensation detonation wave. The experiment was organized such that a supersaturated carbon vapor was formed as a result of the rapid chemical reactions proceeding behind the front of a shock wave. Thus, it is precisely the shock wave that initiated the formation of vapor and its subsequent "explosion" condensation accompa-

Joint Institute of High Temperatures, Russian Academy of Sciences, 13/19 Izhorskaya Str., Moscow 125412, Russia; email: eremin@ihed.ras.ru. Translated from Inzhenerno-Fizicheskii Zhurnal, Vol. 83, No. 6, pp. 1130–1141, November–December, 2010. Original article submitted April 24, 2010.

1062-0125/10/8306-1197

nied by a significant heat release. This complex of processes, unlike the "physical condensation" described by Landau [5], can be called the "chemical condensation."

The present work is based on the recent results of the authors, obtained in [6], where the phenomenon of a significant heating of a reacting mixture by the heat released as a result of the condensation of the carbon vapor formed in the shock-wave pyrolysis of the carbon suboxide C_3O_2 was investigated. The carbon suboxide is a fairly unstable volatile substance whose molecules, when heated to 1400–1600 K, rapidly disintegrate with the formation of a carbon atom and two CO molecules. The heat balance of the transformation of the carbon suboxide into the condensed carbon and CO is somewhat lower than that of acetylene (1):

$$C_3O_2 \rightarrow C(\text{graphite}) + 2CO \quad (+142\ \text{kJ/mole}) , \tag{2}$$

however, an important feature of process (2) is that the limiting stage ("narrow neck") of the growth of the condensed particles is the reaction of formation of carbon vapor, the rate of which increases exponentially with increasing temperature [7]. At a temperature of 1800–2500 K and a pressure of 3–30 atm, the stage of growth of the clusters to the sizes 10^3–10^4 atoms, accompanied by an active heat release, lasts approximately 1–10 μs [8]. The indicated characteristics of the shock-wave pyrolysis of the carbon suboxide allowed the supposition that, under corresponding conditions, the condensation process and the energy release can proceed in the regime of thermal explosion with the formation of a detonation wave.

Another important feature of the decomposition of C_3O_2 and the subsequent condensation of carbon is the complete absence of secondary gaseous reactions (only CO that is chemically stable at temperatures $T < 4000$ K remains in the system). This fact makes it possible to simply determine the interrelation between the growth of the clusters and the heat release behind shock waves different in intensity. The data obtained allowed us to estimate the threshold parameters of formation of a detonation wave. However, to reliably support the existence of this phenomenon, it was necessary to measure the changes in the parameters of a shock wave at different concentrations of C_3O_2.

In [9], we carried out the first preliminary experiments on the strengthening of a shock wave in a mixture containing 10% of C_3O_2 in argon, the results of which have shown that conditions necessary for the formation of a stable detonation can be realized. We were the first to record, in [10], the detonation-wave regimes with parameters close to the Chapman–Jouguet ones.

In the present work, on the basis of the indicated preliminary results, the process of formation of a detonation wave as a result of the chemical condensation of carbon was investigated in more detail and the features of this process in the carbon suboxide and acetylene were analyzed, with particular attention being given to the analysis of the interrelation between the kinetics of the condensation and the heat release under these conditions.

1. Experimental. The experiments were carried out in a high-pressure shock tube of inner diameter 70 mm with an investigation section of length 4.5 m. We investigated the propagation of the reflected shock waves in mixtures containing 10–30% C_3O_2 or C_2H_2 in Ar. Prior to the beginning of the chemical transformations, the temperature and pressure behind the reflected shock wave (the "frozen" parameters) were varied within the wide ranges 1300–2900 K and 4–30 atm. The actual pressure and the velocity of the shock wave were measured by several piezoelectric transducers installed at different distances: 0–300 mm, from the end of the shock tube. For continuous recording of the process of propagation of a shock wave, the tube was equipped with two rectangular sapphire windows of size 160 × 5 mm, the edge of which was located at a distance of 25 mm from the tube end. Through these windows, time-resolved images of the radiation behind the shock wave were recorded in the range 300–800 nm with the use of an ICCD camera (Streak-Star II, LaVision GmbH). In addition, through the indicated windows, the extinction of the laser radiation, reflecting the formation of condensed particles, was recorded at λ = 633 nm at different distances from the tube end. Figure 1 presents the diagram of an experimental setup and the scheme of a diagnostic technique.

A scan of the radiation behind the shock wave in the mixture 1% C_6H_6 + Ar at a temperature T_5 = 2800 K, recorded with the use of the ICCD camera and pressure transducers in a test experiment, is shown in Fig. 2. Under the conditions of this experiment, the pyrolysis of benzene and the formation of carbon nanoparticles proceed very rapidly (in ~10 μs), and then any marked heat effects do not arise. Therefore, it is well seen that the shock wave propagates with a constant velocity and the radiation field behind the wave is fairly uniform. Thus, as the results of this test measurement show, the changes in the velocity of the shock wave and the inhomogeneities of the radiation field,

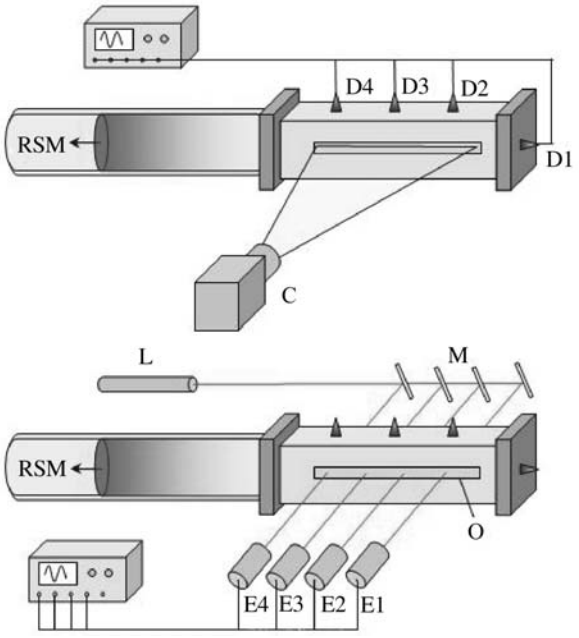

Fig. 1. Diagram of a shock tube and scheme of a multichannel diagnostics of the formation of a detonation behind the reflected shock wave (RSW) with the use of pressure transducers (D1–D4), of a time scann of radiation with the use of rectangular sapphire windows (W) and an ICCD camera (C), and of a measurement of the laser extinction and the self-radiation of the flow with the use of a continuous helium–neon laser (L), a system of mirrors (M), and photomultiplier tubes (E1–E4).

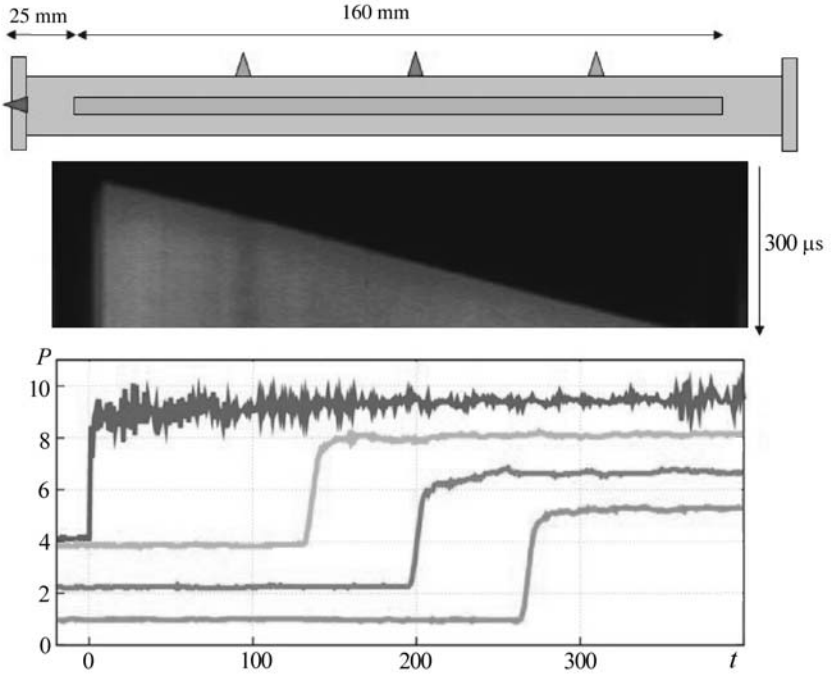

Fig. 2. Diagram of the investigation section of the shock with sapphire windows; time scan of the radiation behind the shock wave in the test mixture 1% C_6H_6 + Ar at a temperature T_5 = 2800 K; records of the pressure transducers for this mixture. P, bar; t, μs.

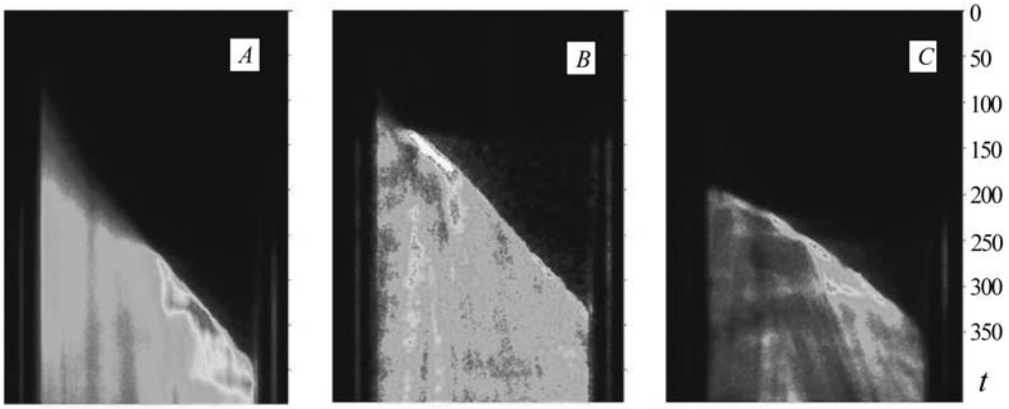

Fig. 3. Time scans of the radiation behind the front of the shock wave in the mixtures initially containing 10 (A), 20 (B), and 30% C_3O_2 (C) in argon at T_5 = 1650 K and V_5 = 1100 m/s (A), T_5 = 1530 K and V_5 = 1050 m/s (B), and T_5 = 1490 K and V_5 = 1100 m/s (C).

detected in the indicated reacting mixture, are caused not by the defects of the experiment but by the heat-release effects occurring in the processes being investigated.

In addition to the direct measurements carried out directly in the process of propagation of a shock wave, particles formed during the experiments were investigated with the use of a Phillips CM-30 electron microscope. The particle-size distribution was investigated at a low resolution with a magnification coefficient m = 45,000. The morphology and structure of the particles was examined at a high resolution with magnification m = 400,000 and 490,000. The microdiffraction of the particles was measured to determine the degree of their crystallization. To determine the percent ratio between the contents of hydrogen and carbon in the particles formed, we have performed an elementary analysis of them on a CHNS-E13 apparatus (Elementar Vario).

2. Results of Measurements. The most informative patterns of the condensation of particles and the formation of a detonation wave in the mixtures being investigated have been obtained with the use of the ICCD camera. Figure 3 shows a time scan of the radiation behind the shock waves in the mixtures initially containing 10, 20, and 30% C_3O_2 in argon. It is well seen that, in these cases, the character of propagation of a shock wave and the flow behind it differ radically from those in the test mixture shown in Fig. 2. In the indicated experiments, the initial "frozen" pressures behind the reflected shock wave comprised 4–8 atm, and the "frozen" temperatures were so low in all of the cases that it has been impossible to detect the radiation of the mixture prior to the heat-release processes. In the first case (Fig. 3A), in the 10% mixture, a condensation wave, accompanied by a radiation, overtakes the front of the shock wave in the region of the center of the window and accelerates it from V_5 = 1050 to 1300 m/s. In the mixture containing 20% C_3O_2 (Fig. 3B), despite the smaller "frozen" temperature, the condensation wave overtakes the shock-wave front much earlier; instantaneously a bright radiation peak is formed at the wave front and, subsequently, the velocity of the shock wave remains unchanged and equal to ~1500 m/s (at an initial value of V_5 = 1025 m/s). The behavior of a shock wave in the mixture containing 30% C_3O_2 is even more surprising (Fig. 3C): initially, this wave accelerates to 1600 m/s (from V_5 = 1100 m/s) and then it slows down to 1300 m/s.

Such behavior of a shock wave was detected with the use of pressure transducers and was investigated by records of the intrinsic emission of a mixture and of the laser extinction at different cross sections of the shock tube, made with the use of a photomultiplier tube. In Fig. 4, the time profiles of the pressure, radiation, and extinction, measured in the mixture containing 10% C_3O_2 at different distances from the end of the shock tube at two different intensities of the initiating shock wave, are compared. The oscillograms A in Fig. 4 were recorded under conditions where reactions were completely absent (T_5 = 1390 K); it is seen from these oscillograms that the pressure P_5 and the velocity of the shock wave are constant and that radiation and extinction signals are absent. The oscillograms B were recorded at a higher temperature T_5 = 1620 K. In this case, the shock wave accelerates, which leads to an increase in the pressure, the appearance of radiation peaks, and to an increase in the extinction rate, reflecting the formation of condensed particles.

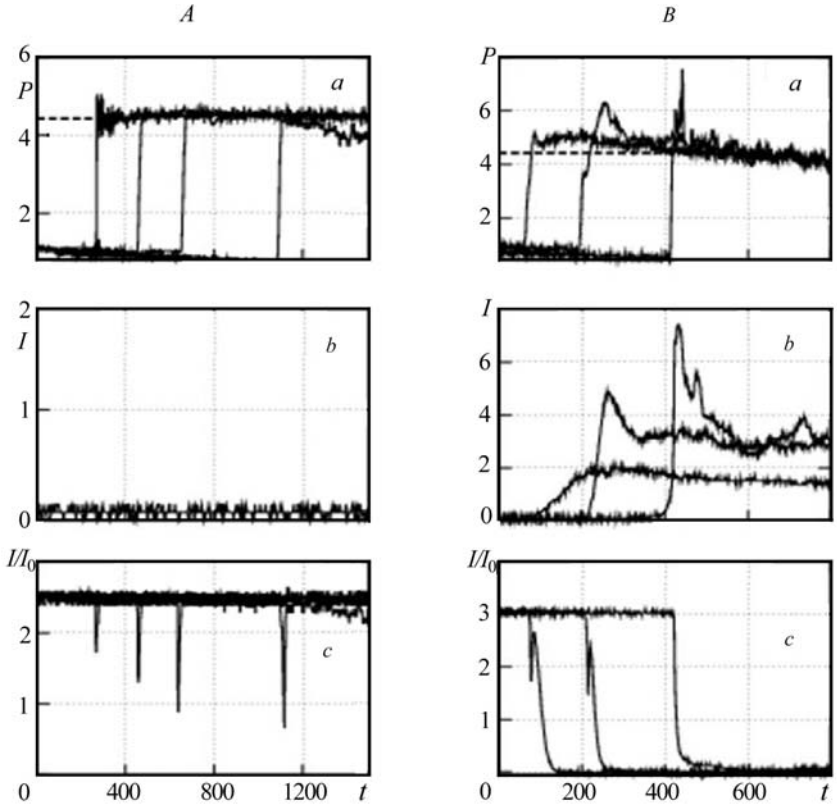

Fig. 4. Time profiles of the pressure (a), radiation intensity (b), and the extinction (c) measured in the mixture 10% C_3O_2 + Ar at different distances (70, 140, and 295 mm) from the end of the shock tube at T_5 = 1390 (A) and 1620 K (B). *P*, bar; *t*, μs; *I*, rel. units.

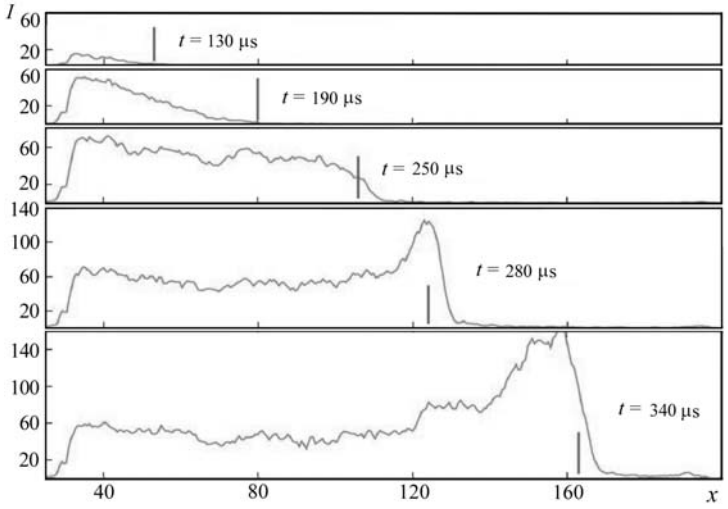

Fig. 5. Records of instantaneous distributions of the radiation intensity along the length of the shock tube obtained with the use of the ICCD camera for the experiment shown in Fig. 3A. The vertical lines indicate the positions of the shock-wave front. *I*, rel. units; *x*, mm.

The most expressive pattern of gradual development of a detonation structure was detected for the mixture 10% C_3O_2 in argon at T_5 = 1650 K (see Fig. 3A). Figure 5 presents several instantaneous distributions of the radiation intensity behind the front of a shock wave, constructed on the basis of the measurement data. The position of the

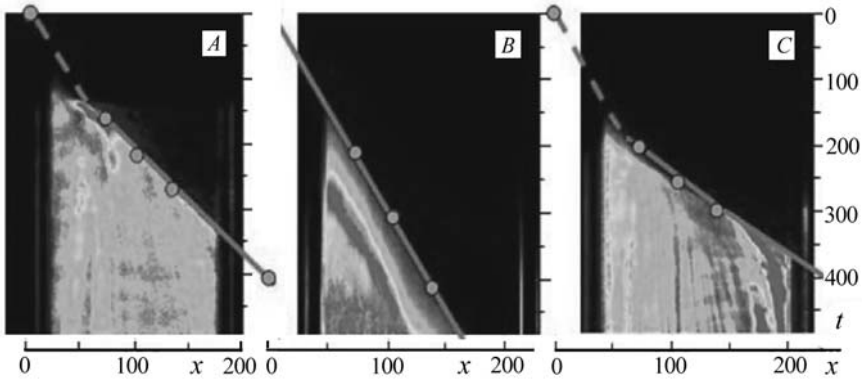

Fig. 6. Comparison of the scans of the radiation behind the front of the shock wave in the mixtures initially containing 20% C_3O_2 (A) and 20% C_2H_2 (B, C) in argon at P = 7.5 (A), 6 (B), and 30 bar (C). The red line denotes the trajectory of the shock-wave front determined by the indications (green points) of the pressure transducers. t, μs; x, mm.

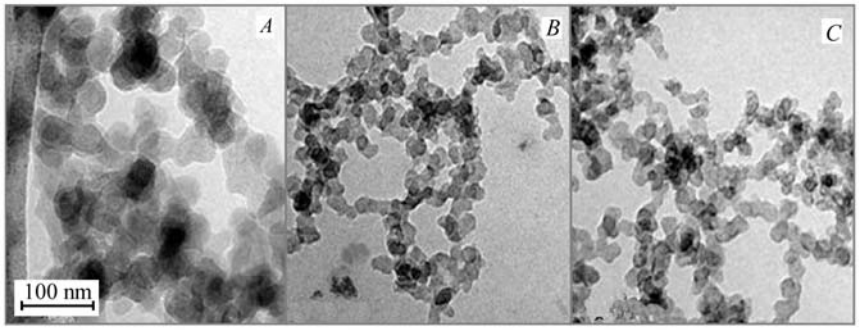

Fig. 7. Electron-microscope images of carbon nanoparticles in the mixtures 20% C_3O_2 + Ar (A) and 20% C_2H_2 + Ar (B, C).

wave front denoted by the vertical line was determined by the measurements of the pressure transducers. It is well seen that the radiation intensity begins to increase near the end of the shock tube at the instant the wave front has moved to a distance of 55 mm from the tube end. Then the growing radiation wave gradually overtakes the front of the shock wave.

Finally, at a distance of more than 120 mm from the end of the shock tube, the radiation overtakes the front of the shock wave and a typical distribution of the detonation-radiation intensity is formed. A comparison with the oscillograms (Fig. 4) measured under very close conditions has shown that the sharp increase in the radiation intensity is completely due to the rapid heat release accompanying the condensation shock.

In Fig. 6, the radiation scans recorded under similar conditions for C_3O_2 and acetylene are compared. The scan shown in Fig. 6A presents the formation of a detonation wave in C_3O_2 at an initial pressure, equal to 7.5 atm, behind the shock-wave front. It is well seen that, at the beginning of the observation zone, the condensation wave (heating the medium and enhancing its radiation) overtakes the front of the shock wave, enhances and accelerates this wave, and forms a detonation structure with radiation and pressure peaks at its front. However, unlike C_3O_2, in acetylene, at a close initial pressure equal to 6 atm (see Fig. 6B), the condensation wave manifesting itself pronouncedly by the intensive heating of the mixture is separated from the wave-front by a fairly broad zone (about 50 mm) that does not change with time. In other words, under the indicated conditions, a condensation wave exerts no influence on the initiating shock wave, which continues to move with a constant velocity. When the pressure in the indicated mixture increases to 30 atm (Fig. 6C), the pattern changes radically — the condensation wave quickly overtakes the shock wave, accelerates it, and forms a detonation-like structure that is very similar to that detected earlier for C_3O_2.

3. Properties of the Carbon Particles Obtained. In all the experiments carried out by us, a fairly large number of condensed particles were deposited on the walls of the shock tube. Figure 7 shows typical images of the carbon

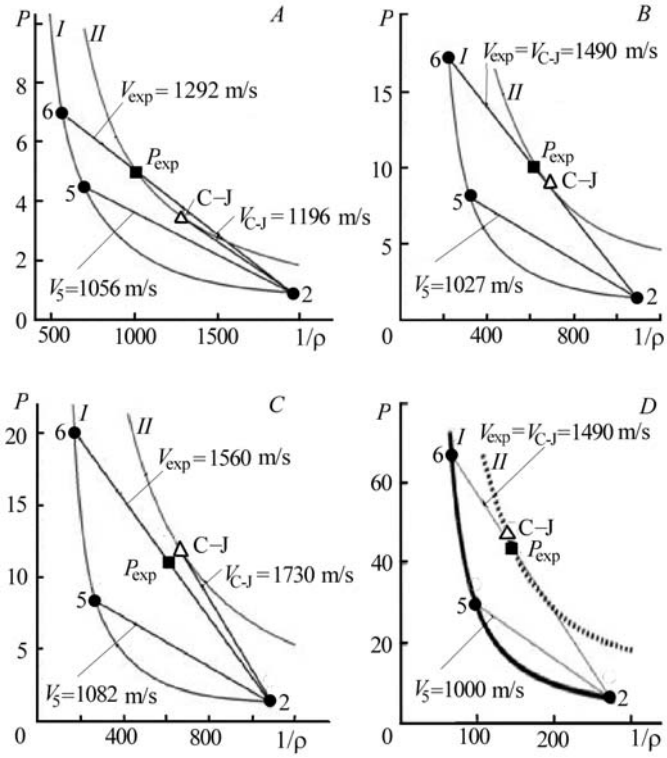

Fig. 8. Hugoniot adiabats and detonation regimes for the initial mixtures (curves I) and for the mixtures after the condensation (curves II): A) mixture 10% C_3O_2 + Ar, T_{C-J} = 2050 K; B) mixture 20% C_3O_2 + Ar, T_{C-J} = 2460 K; C) mixture 30% C_3O_2 + Ar, T_{C-J} = 2830 K; D) 20% C_2H_2 + Ar, T_{C-J} = 2517 K. Points 2 denote the initial states of the mixtures before the shock wave, points 5 denote the frozen parameters behind the shock wave, points 6 denote the peak values of the pressure behind the accelerated wave, P_{exp} is the steady-state pressure behind the shock wave, the points C–J denote the Chapman–Jouguet parameters. P, bar; $1/\rho$, cm^3/g.

particles obtained. In the hydrogen-free mixture of 20% C_3O_2 + Ar (Fig. 7A), the particles have a fairly large size — their average diameter is equal to 30 nm, while the size of the particles in the mixture 20% C_2H_2 + Ar (Fig. 7B and C) is markedly smaller — their average diameter is 19.3 nm. The measurements carried out with a high resolving power have shown that the particles in C_3O_2 are completely amorphous, while the nanoparticles formed in the acetylene mixture were crystallized to some degree.

An analysis of the relative content of carbon and oxygen in the condensed particles has shown that they consist practically completely of carbon; for all the mixtures, the maximum content of hydrogen in these particles was smaller than the measurement-error limit (~0.3%).

4. Analysis of the Results Obtained. *4.1. Estimation of the detonation parameters in the mixtures being investigated.* To estimate the relation between the parameters of the shock waves, propagating in the mixtures being investigated under the action of the energy of the chemical condensation of the carbon vapor, and the detonation parameters, we compared the measured values of the velocity of a shock wave and the pressure behind its front with the calculations of the Hugoniot adiabats for these mixtures [11]. Figure 8 shows results of calculations of the indicated adiabats for the initial mixtures (curves I) and for the mixtures after the condensation (curves II). The straight lines 2–5 correspond to the calculated velocities of the reflected shock wave. Points 6 and rays 2–6 represent the experimentally measured maxima of the pressures at a radiation peak and the velocity of the front of the shock wave after its acceleration. The points P_{exp} show the values of the steady-state pressure, and the points C–J demonstrate the parameters of the Chapman–Jouguet detonation calculated in the one-dimensional approximation [11]. It is seen that, in the mixture 10% C_3O_2 + Ar (Fig. 8A), ray 2–6 intersects adiabat I at markedly higher pressures than P_{exp} and the wave

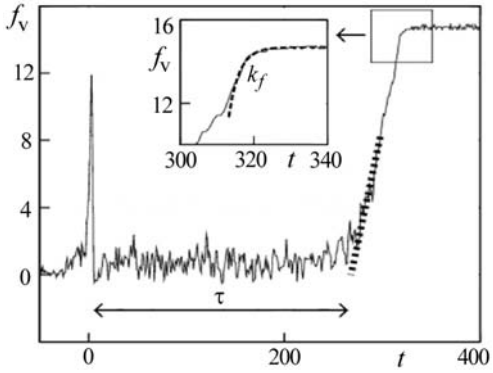

Fig. 9. Typical time profile of a volume fraction of the condensed carbon determined by the signal of attenuation of the probing laser radiation (see (4)) in the pyrolysis of C_2H_2 behind the shock wave in the mixture 20% C_2H_2 +Ar and results of its processing. The temperature and pressure behind the shock wave comprise 1562 K and 6.21 atm. f_v, ppm; t, ms.

velocity measured is much higher than the Chapman–Jouguet velocity (tangent to curve II from point 2). Such behavior of the shock wave can be due to the insufficient heat release, which additionally supports the pressure wave arising behind the shock wave. This flow regime is usually called the "overcompressed detonation." The calculation and measurement data on the pressure and shock-wave velocity obtained for the mixture 20% C_3O_2 + Ar are in very good agreement (Fig. 8B). Under these conditions, the calculated temperature behind the detonation front was 2460 K, which, according to [12], is close to the temperatures at which maximum condensation rates are attained. For the richer mixture 30% C_3O_2 + Ar (Fig. 8C), the measured values of the pressure and shock-wave velocity are smaller than the calculated ones. This fact can be explained by the excess heat release leading to an incomplete condensation at temperatures higher than 2800 K. At these temperatures, the reverse processes of disintegration of particles, decreasing the effective condensation rate, begin to act. Because of this, the condensation energy cannot be completely transformed into the dynamic energy of the shock wave, and the so-called "overcompressed" (decaying) detonation takes place.

Figure 8D presents the Hugoniot adiabats calculated for the mixture 20% C_2H_2 + Ar at an initial pressure of 30 atm behind the shock wave (see Fig. 6C). It is well seen that, by analogy with the mixture 20% C_3O_2 + Ar, at an initial pressure of 7.5 atm (Fig. 8B), the flow regime detected agrees well will the calculation Chapman–Jouguet parameters.

Thus, our investigation has shown that, even though a detonation wave is formed in both mixtures, the limiting pressure at which a detonation arises is much higher for acetylene than for C_3O_2, despite the fact that the heat released as a result of reaction (1) is much greater than the heat from reaction (2). It is apparent that the main reason for the distinction between the processes of formation of a detonation wave in C_2H_2 and C_3O_2 is the difference between the rates of heat release in them, and, for analysis of the indicated process, it is necessary to investigate the features of the kinetics of condensation of carbon in the process of pyrolysis of these substances.

4.2. Kinetics of chemical condensation of carbon in the pyrolysis of C_2H_2 and C_3O_2. The information on the kinetics of the condensation investigated in our experiments was mainly obtained from the time profiles of attenuation (extinction) of the laser radiation, i.e., the ratio I/I_0 between the intensity of the transmitted radiation I and the intensity of the incident radiation I_0. The amplitude of the corresponding signals allows one to determine the volume fraction of the condensed phase f_v:

$$f_v = -\frac{\ln I/I_0}{\varepsilon l}\,, \tag{3}$$

where $\varepsilon = 5.1 \cdot 10^6$ m^{-1} (for 633 nm [13]) and $l = 0.07$ m. The time change in f_v determines two quantities — the induction period of the beginning of the condensation τ and the effective rate constant of the condensation process k_f. Figure 9 shows a typical time profile of a volume fraction of the condensed phase f_v in acetylene behind the shock wave. The radiation peak arising at the instant of passage of the shock-wave front is due to the deviation of the laser

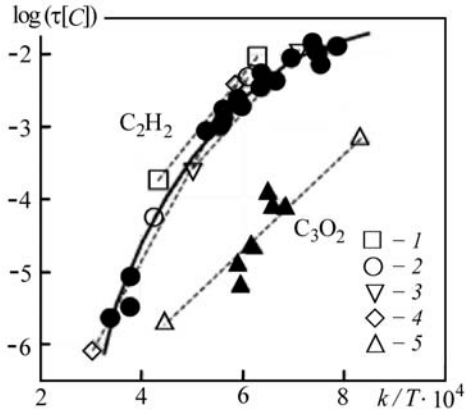

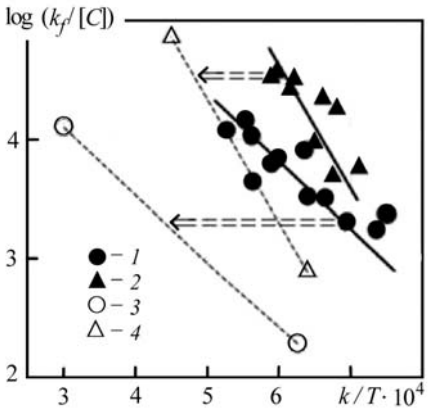

Fig. 10. Comparison of the induction periods measured in C_2H_2 and C_3O_2 in the present work with the corresponding data obtained in previous works for the more diluted mixtures: 1) 5% C_2H_2 [14]; 2) (0.2–1%) C_2H_2 [15]; 3) 2% C_2H_2 [16]; 4) 10% C_2H_2 [17]; 5) (0.03–1%) C_3O_2 [7]; the solid curve is an approximation of the data of the present work. log (τ[*C*]), mole·s/m^3.

Fig. 11. Comparison of the condensation-rate constants measured in C_2H_2 (1) and C_3O_2 (2) with the corresponding data obtained for the diluted mixtures: 3) (0.03–3%) C_3O_2 [7]; 4) (0.2–1%) C_2H_2 [15]. The horizontal rows points to the possible shift of the actual temperature of the mixture because of the thermal condensation effects. log (k_f[*C*]), m^3/(mole·s).

beam caused by the density gradient. After the passage of the shock wave, a prolonged induction period, determined as the time interval between the passage of the shock-wave front and the point of intersection of the tangent to the profile of the signal at the point of its maximum inclination to the time axis, takes place. Then the condensed phase sharply increases, and the rate of this increase is determined by the extrapolation of the later stages of the process by the relaxation equation

$$\frac{df_v}{dt} = k_f \left(f_v^{\infty} - f_v \right) . \tag{4}$$

Results of our measurements of the quantities τ and k_f in the rich mixtures with 20–30% of condensed molecules, compared to the data of measurements carried out in the previous works with the use of more diluted mixtures, are presented in Figs. 10 and 11. All these data are related to the total concentration of the condensed carbon and are presented in the Arrhenius coordinates as functions of the initial temperature behind the shock wave, determined without regard for the heat effects of the pyrolysis and condensation processes. Figure 10 shows the induction periods in acetylene and C_3O_2. It is seen that all the results of the present work are in fairly good agreement with the results of the previous measurements, but, what is most important, the induction period of growth of particles in C_2H_2 is larger by almost two orders of magnitude than that in C_3O_2 throughout the measurement range.

The data on the condensation rate (Fig. 11) are entirely different. The rates of condensation of particles in the rich mixtures, related to the initial temperature behind the shock wave, are much higher than those measured in the poor mixtures. Moreover, it is seen that the condensation rate measured in acetylene is slightly lower than that in C_3O_2.

Actually, the most important difference between the mechanism of formation of the condensed carbon in the pyrolysis of the hydrogen-free precursor of C_3O_2 and the mechanism of formation of soot in the pyrolysis of any hydrocarbons is that the primary products of the C_3O_2 decomposition are carbon atoms and C_2 radicals [13–18]:

$$C_3O_2 + M \rightarrow C_2O + CO + M ,$$

$$C_2O + M \rightarrow C + CO + M ,$$

$$C_3O_2 + C \rightarrow C_2 + 2CO\,, \tag{5}$$

$$C_2O + C_2O \rightarrow C_2 + 2CO\,,$$

$$C_2O + C \rightarrow C_2 + CO\,.$$

Therefore, the further growth of the carbon clusters and the formation of condensed nanoparticles begins directly with the pyrolysis reaction and is realized through the surface growth

$$C_n + C \rightarrow C_{n+1}\,, \tag{6}$$

or through the coagulation of small clusters

$$C_n + C_m \rightarrow C_{n+m} \tag{7}$$

with rates comparable to the frequency of the gas-kinetic collisions [19].

The numerical calculations of the kinetics of dissociation of C_3O_2 and the subsequent condensation of carbon vapor with account for the energy balance in each reaction were carried out with the use of the kinetic scheme proposed in [20]. An approximate dependence of the heat balance of this process on the particle size is presented in Fig. 12.

Unlike C_3O_2, the pyrolysis of acetylene as well as of any other hydrocarbons does not directly lead to the appearance of carbon clusters. For example, in [21], as the primary reactions of the acetylene pyrolysis, the reactions of detachment of a hydrogen atom

$$C_2H_2 + M \rightarrow C_2H + H + M \tag{8}$$

or the reaction of polymerization of C_2H_2

$$C_2H_2 + C_2H_2 \rightarrow C_4H_3 + H \tag{9}$$

under different pyrolysis conditions were considered. During the further reactions, complex hydrocarbon radicals form polyacetylenes [22, 23] or polyaromatic structures [23, 24].

In any event, the complex hydrocarbon molecules formed at this stage of the process are most probably transparent for the probing laser radiation at 633 nm, and it is precisely this stage that reflects the prolonged period of induction in acetylene mixtures. Since the induction periods measured in these experiments in relation to the "frozen" temperature T_5 are in good agreement with the data obtained for the diluted mixtures (see Fig. 10), it may be concluded that the heat release at this stage of the process is insignificant and the temperature of the mixture does not differ markedly from the initial values of T_5.

The further stages of the process, characterized by the formation of carbon particles nontransparent at 633 nm, point to the fact that the measured condensation rates differ substantially from the corresponding data of the previous works (Fig. 11). It is most natural to suggest that the detected difference between the rates of growth of particles in C_2H_2 and C_3O_2 and in the diluted mixtures is due to the significant heat release at this stage of the process, causing an increase in the temperature of the mixture. Simple estimations of the heat effects of reactions (1) and (2) have shown that the increase in the mixture temperature can reach 500 K for C_3O_2 and 800–1000 K for C_2H_2. The arrows in Fig. 11 show the shift of the obtained values of k_f, caused by the increase in the real temperature of the mixture. It is not difficult to see that, in this case, they agree well with the measurement data obtained for the poor mixtures.

4.3. Thermodynamics of the condensation in the process of decomposition of C_3O_2 and C_2H_2. The thermodynamic processes arising as a result of the decomposition of C_3O_2 and the subsequent condensation of carbon were analyzed on the basis of recent data on the heat effects occurring in the process of formation of carbon nanoparticles in the shock-wave pyrolysis of C_3O_2 [6]. The integral heat effect Q of the reaction

$$C_3O_2 \rightarrow 2CO + C_N/N \tag{10}$$

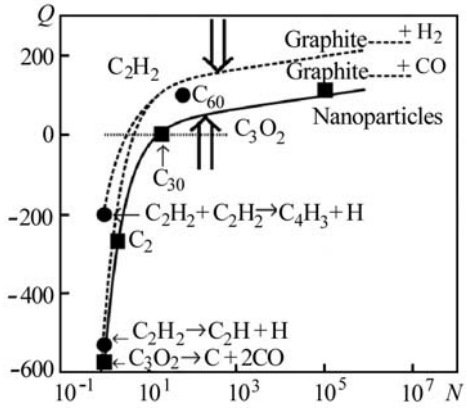

Fig. 12. Approximate dependences of the integral heat balance of the processes $C_2H_2 \rightarrow H_2 + (2/N)C_N$ and $C_3O_2 \rightarrow 2CO + (1/N)C_N$ on the number of particles N in a cluster. Q, kJ/mole.

was calculated from the equation

$$Q = \Delta H_f(C_3O_2) - 2\Delta H_f(CO) - \Delta H_f(C_N)/N \ , \tag{11}$$

where ΔH_f is the enthalpy of formation of the mixture components.

The main indeterminacy in the calculations was due to the lack of reliable data on the state and enthalpy of the different-sized carbon nanoparticles formed. Figure 12 presents approximate dependences $Q = f(N)$ constructed on the basis of the data taken from [6, 25, 26]. In accordance with these data, the energy expended for the dissociation of C_3O_2 (~573 kJ/mole) is compensated for even at a cluster size of $N \approx 20$ atoms, and the process becomes exothermic when the clusters grow further. It is seen from Fig. 12 that when the size of the final particles is about 20 nm (corresponding to $N \approx 10^6$ atoms in the case where the density of particles is $1.86 \cdot 10^3$ kg/m^{-3} [27]), the heat effect of the reaction $C_3O_2 \rightarrow 2CO + (1/N)C_N$ approaches ~100–120 kJ/mole.

It is even more difficult to calculate the energy balance of different stages of the pyrolysis of acetylene because of the enormous number of intermediate stages of growth of polycyclic hydrocarbons, the thermodynamics of which is as yet imperfectly understood. Therefore, the dependences $Q = f(N)$ presented by the dotted lines in Fig. 12 should be considered as rough estimations of the thermodynamics of the $C_2H_2 \rightarrow H_2 + (2/N)C_N$ process that pretend in no way to be a correct representation of this process in the region $2 < N < 10^3$. The two initial values of the indicated dependences correspond to the two different primary pyrolysis reactions (8) and (9).

The heat effects of the subsequent polymerization reactions are poorly understood. It is only known that the exothermic efficiency of the process of "coiling" of linear acetylene radicals in a benzene ring is fairly high [28]:

$$C_2H_2 \rightarrow 1/3C_6H_6 \quad (+ 200 \text{ kJ/mole}) \ , \tag{12}$$

however, the discussion on the role of these processes in the acetylene pyrolysis up till now has not given definite conclusions [23, 24].

In any event, it may be suggested that the growing polycyclic hydrocarbons gradually lose hydrogen atoms and, in doing so, take on the properties of carbon particles in the case where $N_H < 0.1N_C$ and $N_C > 10^3$. It is precisely these dimensions of the particles at which their refraction index is substantially increased, and this increase manifests itself as a sharp increase in the extinction at λ = 633 nm. This region of particle sizes is denoted by the vertical arrows in Fig. 12. In the pyrolysis of C_3O_2, the hydrogen-free carbon particles have a somewhat larger refraction index [7, 12, 29]; therefore, the extinction begins to grow at smaller sizes of the carbon particles.

Conclusions. The amplification of a shock wave and its transformation into a detonation wave as a result of the energy release in the chemical condensation of carbon in the process of thermal decomposition of the carbon suboxide and acetylene behind the shock waves were experimentally investigated in detail. The estimates made within the framework of the one-dimensional detonation theory allowed the conclusion that a detonation wave with parameters

corresponding well to the calculated Chapman–Jouguet parameters can arise both in acetylene and C_3O_2, and the limiting pressure of appearance of a detonation in acetylene is much higher than that in C_3O_2.

An analysis of the energy balance of the processes occurring behind the shock waves in the indicated mixtures has supported the conclusion that the stages of growth of particles, detected by the increase in the extinction, are accompanied by a significant heat release (Fig. 12) and the corresponding condensation rates are fairly high — the characteristic heat-release times comprise 10^{-5}–10^{-6} s (see Fig. 11). Moreover, the great heat release at this stage of the reaction causes an additional self-acceleration of the process.

Thus, it may be concluded that the main reason for the deceleration of the formation of a detonation wave in acetylene, as compared to that in the carbon suboxide, is not the difference between the rates of condensation of carbon particles in these compounds but the prolonged period of induction of growth of the condensed particles during which the complex hydrocarbon molecules are polymerized. This stage of the process is not accompanied by a marked heat release; however, it spatially separates the front of the shock wave and the condensation zone and, in doing so, prevents the action of the hot layers of the mixture on the shock-wave parameters. An increase in the pressure and, accordingly, in the concentration of the reacting particles leads to a narrowing of this zone and to a decrease in the rate of its heating from the heat-release zone side. A further increase in the temperature of the compound leads to a sharp decrease in the induction time (see the solid line in Fig. 10) and to the collapse of the whole process with the formation of a detonation wave.

The authors express their gratitude to Prof. H. Wagner and Dr. H. Jander (Göttingen University) for fruitful discussions and Dr. I. Deppe (LaVision, GmbH) for providing of the measurements with the use of an ICCD camera. This work was carried out with financial support from the Russian Foundation for Basic Research (grants 09-03-00648-a, 08-03-91955-NNIO-a) and the Program of the Presidium of the Russian Academy of Sciences "Thermal Physics and Mechanics of Extremum Energy Actions and Physics of Strongly Compressed Substances."

NOTATION

$[C]$, concentration of carbon atoms; f_v^∞, f_v, final and current volume fractions of the condensed carbon fraction; ΔH_f, enthalpy of formation of components of a mixture; I_0, I, intensities of the incident and transmitted laser radiation; k_f, rate constant of growth of carbon nanoparticles; l, absorption length (diameter of the shock wave); m, magnification factor of an electron microscope; N, N_C, N_H, number of atoms in a cluster, in a carbon cluster, and in a polycyclic-carbon cluster; P_{exp}, experimental pressure behind the detonation wave; Q, heat effect of a reaction; T_2, T_5, T_{C-J}, "frozen" temperatures behind the incident and reflected shock waves and the temperature at the Chapman–Jouguet point; t, current time of development of processes measured from the instant a shock wave is reflected from the end of the shock tube; V_5, velocity of the reflected shock wave in the laboratory coordinate system; x, distance from the end of the shock tube; ε, coefficient of absorption of carbon nanoparticles; λ, wavelength of the laser radiation; ρ, volume density of a mixture; τ, induction period. Subscripts: v, volume; exp, experimental.

REFERENCES

1. B. A. Ivanov, *The Physics of Acetylene Explosion* [in Russian], Khimiya, Moscow (1969).
2. M. Berthélot and H. L. Le Chatelier, Sur la vitesse de detonation da l'acetylene, *Comptes Rendus*, **129**, No. 2, 427–434 (1899).
3. E. Penny, The velocity of detonation of compressed acetylene, *Disc. Faraday Soc.*, **22**, 157–161 (1956).
4. V. G. Knorre, M. S. Kopylov, and P. A. Tesner, The role of soot in acetylene detonation, *Fiz. Goreniya Vzryva*, **13**, No. 6, 863–867 (1977).
5. L. D. Landau and E. M. Lifshits, *Theoretical Physics* [in Russian], in 10 vols., Vol. 6, *Hydrodynamics*, Fizmatlit, Moscow (2001).
6. A. V. Emelianov, A. V. Eremin, A. A. Makeich, H. Jander, H. G. Wagner, R. Starke, and C. Schulz, Heat release of carbon particle formation from hydrogen-free precursors behind shock waves, *Proc. Combust. Inst.*, **31**, 649–656 (2007).

7. K. J. Doerge, D. Tanke, and H. G. Wagner, Particle formation in carbon suboxide pyrolysis behind shock waves, *Z. Phys. Chem.*, **212**, 219–229 (1999).
8. A. Emel'yanov, A. Eremin, and H. G. Wagner, Temperature dependence of the rate of formation of carbon nanoparticles in pyrolysis behind shock waves, *Khim. Fiz.*, **23**, 62–71 (2004).
9. A. V. Emel'yanov, A. V. Eremin, A. A. Makeich, and V. E. Fortov, Formation of a condensation detonation wave, *Pis'ma Zh. Éksp. Teor. Fiz.*, **87**, Issue 9, 556–559 (2008).
10. A. V. Emelianov, A. V. Eremin, V. E. Fortov, H. Jander, A. A. Makeich, and H. G. Wagner, Detonation wave driven by condensation of supersaturated carbon vapor, *Physical Review E*, **79**, 035303 (1–4) (2009).
11. I. N. Zverev and N. N. Smirnov, *Combustion Gas Dynamics* [in Russian], Izd. MGU, Moscow (1987).
12. A. Emelianov, A. Eremin, H. Jander, A. Makeich, P. Roth, R. Starke, and H. G. Wagner, Time and temperature dependence of carbon particle growth in various shock wave pyrolysis processes, *Proc. Combust. Inst.*, **30**, 1433–1440 (2005).
13. S. C. Lee and C. L. Tien, Optical constants of soot in hydrocarbon flames, in: *Proc. Combust. Inst.*, **18**, 1159–1166 (1981).
14. Y. Yoshizawa, H. Kawada, and M. Kurokawa, A shock wave study on the process of soot formation from acetylene pyrolysis, in: *Proc. Combust. Inst.*, **17**, 1375–1381 (1979).
15. V. G. Knorre, D. Tanke, Th. Thienel, and H. G. Wagner, Soot formation in the pyrolysis of benzene/acetylene and acetylene/hydrogen mixtures at high carbon concentrations, in: *Proc. Combust. Inst.*, **26**, 2303–2310 (1996).
16. D. E. Fussey, A. J. Gosling, and D. Lampard, A shock-tube study of induction times in the formation of carbon particles by pyrolysis of the C_2 hydrocarbons, *Combust. Flame*, **32**, No. 1, 181–192 (1978).
17. T. Tanzawa and W. C. Gardiner, Jr. Thermal decomposition of acetylene, in: *Proc. Combust. Inst.*, **17**, 563–573 (1979).
18. G. Friedrichs and H. G. Wagner, Investigation of the thermal decay of carbon suboxide, *Z. Phys. Chem.*, **203**, 1–14 (1998).
19. J. Sojka, J. Warnatz, P. A. Vlasov, and I. S. Zaslonko, Kinetics modeling of carbon suboxide thermal decomposition and formation of soot-like particles behind shock waves, *Combust. Sci. Technol.*, **158**, 439–460 (2000).
20. H. G. Wagner, P. A. Vlasov, K. Yu. Derge, A. V. Eremin, I. S. Zaslonko, and D. Tanke, Kinetics of the formation of carbon clusters in the process of C_3O_2 pyrolysis, *Kinetika Kataliz*, **42**, No. 5, 645 (2001).
21. M. Frenklach, S. Taki, M. B. Durgaprasad, and R. A. Matuda, Soot formation in shock-tube pyrolysis of acetylene, allene and 1,3-butadiene, *Combust. Flame*, **54**, No. 1, 81–101 (1983).
22. A. V. Krestinin, Detailed modeling of soot formation in hydrocarbon pyrolysis, *Combust. Flame*, **121**, 513–524 (2000).
23. P. Vlasov and J. Warnatz, Detailed kinetic modeling of soot formation in hydrocarbon pyrolysis behind shock waves, *Proc. Combust. Inst.*, **29**, 2335–2341 (2002).
24. M. Frenklach and H. Wang, Detailed modelling of soot particle nucleation and growth, in: *Proc. Combust. Inst.*, **23**, 1559–1566 (1991).
25. M. W. Chase, Jr., *NIST-JANAF Themochemical Tables*, 4th. ed., Melville, *J. Phys. Chem. Ref. Data*, 1951 (1998).
26. J. M. L. Martin and P. R. Taylor, Accurate *ab initio* total atomization energies of the C_n clusters (n = 2–10), *J. Chem. Phys.*, **102**, 8270–8273 (1995).
27. A. F. Kirk and D. F. Othmer, *Encyclopedia of Chemical Technology*, Vol. 4, 4th ed., John Wiley and Sons (1992).
28. V. I. Babushok and A. W. Miziolek, Combustion flame of acetylene decomposition, *Combust. Flame*, **136**, No. 1, 141–145 (2004).
29. A. Emelianov, A. Eremin, H. Jander, and H. G. Wagner, Spectral and structural properties of carbon nanoparticle forming in C_3O_2 and C_2H_2 pyrolysis behind shock waves, in: *Proc. Combust. Inst.*, **29**, 2351–2357 (2002).